Annals of Glaciology 57(71) 2016 doi: 10.3189/2016AoG71A073

An assessment of basin-scale glaciological and hydrological sensitivities in the Hindu Kush–Himalaya

Joseph M. SHEA,[1] Walter W. IMMERZEEL[1,2]

[1]*International Centre for Integrated Mountain Development, Khumaltar, Kathmandu, Nepal*
[2]*Department of Physical Geography, Faculty of Geosciences, Utrecht University, Utrecht, Netherlands*
Correspondence: Joseph M. Shea <joseph.shea@icimod.org>

ABSTRACT. Glacier responses to future climate change will affect hydrology at sub-basin scales. The main goal of this study is to assess glaciological and hydrological sensitivities of sub-basins throughout the Hindu Kush–Himalaya region. We use a simple geometrical analysis based on a full glacier inventory and digital elevation model to estimate sub-basin equilibrium-line altitudes (ELAs) from assumptions of steady-state accumulation area ratios. The ELA response to an increase in temperature is expressed as a function of mean annual precipitation, derived from a range of high-altitude studies. Changes in glacier contributions to streamflow in response to increased temperatures are examined for scenarios of both static and adjusted glacier geometries. On average, glacier contributions to streamflow increase by ~50% for a +1 K warming based on a static geometry. Large decreases (–60% on average) occur in all basins when glacier geometries are instantaneously adjusted to reflect the new ELA. Finally, we provide estimates of sub-basin glacier response times that suggest a majority of basins will experience declining glacier contributions by 2100.

KEYWORDS: climate change, glacier hydrology

INTRODUCTION

As water towers in one of the most populated regions of the planet, the mountains of high Asia are integral components of regional water budgets (Immerzeel and others, 2010), and mountain water resources contribute to agricultural, economic and social stability (Xu and others, 2009). The contribution of glaciers to streamflow in the region is of particular interest given that they have been primarily losing mass in recent decades, though there are some localized exceptions (Hewitt, 2005; Bolch and others, 2012; Jacob and others, 2012; Kääb and others, 2012; Gardelle and others, 2013). Hydrologically, the long-term loss of glaciers will reduce ice-melt contributions during dry and warm seasons, and increase the interannual variability of higher-order streams in glacierized catchments (Baraer and others, 2012).

The definition of glacier contribution to streamflow is important, and in some studies this is taken to mean the entire contribution of snow and ice melt from glacierized areas. We adopt a narrower definition that includes only meltwater derived from the glacier surface (La Frenierre and Mark, 2014; O'Neel and others, 2014), which is related to the glacier mass balance. The annual mass balance of a glacier is the difference between annual accumulation and annual ablation, which occurs primarily through surface melt in the HKH region. While glacier contributions to streamflow are greatest in negative balance years, positive balance years will still see a substantial glacier contribution. The hypothetical loss of glaciers thus constitutes a significant change to catchment hydrology, and will result in increased streamflow variability and net reductions in flow (Baraer and others, 2012).

The long-term effects of decreased glacier cover on streamflows have been estimated primarily through modeling approaches that use calibrated parameters and a suite of climate change scenarios (Lutz and others, 2014). Scenarios of decadal-scale increases in streamflow in response to climate warming (Immerzeel and others, 2013; Lutz and others, 2014) and overall modest decreases out to the end of the 21st century (Sorg and others, 2012) support the hypothesis of 'peak water' in glacierized catchments (Huss and others, 2014). However, distributed hydrological models require a variety of data for input, calibration and validation, and in many regions of the Hindu Kush–Himalaya (HKH) these data do not exist. Hydrological scenarios must also somehow take into account the transient response of glaciers to climate change (Stahl and Moore, 2006; Marshall and others, 2011; Immerzeel and others, 2012).

Given the difficulties in modeling the transient response of both glaciers and streamflow to climate change in a data-poor region with extreme topographic complexities, a simpler method to examine glacier and streamflow sensitivities to future climate change is desirable. Conceptually, streamflow responses to future climate warming depend on the current glacier distribution, the sensitivity of glaciers to changes in temperature and precipitation, the relative contribution of glaciers to streamflow, and the future climate pathway. In this study, our objectives are threefold: (1) to define and quantify glaciological and hydrological sensitivities of sub-basins throughout the HKH region, (2) to quantify regional changes in future glacier meltwater production and (3) to provide an approximation of glacier response times and hydrological change.

METHODS AND DATA

Future changes in meltwater contribution depend on the sensitivity of glaciers in a basin to climatic change, and glacier sensitivity to climate change is a function of climatological and glaciological settings. The equilibrium-line altitude (ELA) for any glacier defines the elevation

Table 1. Parameter values used in study calculations

Parameter	Description	Unit	Value/range
dM/dZ	Mass-balance gradient below ELA	m.w.e m^{-1}	–0.004 to –0.010
AAR	Steady-state accumulation area ratio	–	0.40 to 0.60

where accumulation processes are balanced by ablation processes (Cogley and others, 2011). Changes in the ELA, due primarily to changes in temperature and precipitation (Kuhn, 1989), will affect the size of the ablation and accumulation areas, and will subsequently affect the contribution of glacier melt to streamflow for glaciers where melt is a significant ablation process. An increase in mean annual temperature, for example, will produce a rise in the ELA as snowmelt rates increase and snowfall totals decrease due to precipitation phase change.

Glaciological sensitivity

We define a glaciological sensitivity S_G (km^2 K^{-1}, or % (relative to original ablation area) K^{-1}) as the change in ablation area (dA) for a given change in ELA (dELA):

$$S_G = \frac{\mathrm{d}A}{\mathrm{dELA}}. \quad (1)$$

Of importance here is the designation of the current ELA. On monsoon-type glaciers, the ELA is typically interpolated from surface mass-balance measurements made over a range of elevations (e.g. Wagnon and others, 2013). End-of-ablation-season snowline elevations can be used as a proxy for ELA (Meier, 1962; Rabatel and others, 2005; Shea and others, 2013), though pervasive cloud cover and simultaneous accumulation and ablation complicate this approach in monsoon-dominated regions (Brun and others, 2014). Alternatively, a theoretical steady-state ELA (ELA$_0$), that defines the ELA corresponding to net mass balance of zero, can be estimated from glacier area–altitude distributions (Benn and Lemkuhl, 2000). The ratio between the accumulation area and the total area (accumulation area ratio (AAR)) can be used to estimate a steady-state ELA.

AARs of 0.6 have previously been assumed for many Himalayan regions (Porter, 1970; Williams,1983; Burbank and Cheng, 1991; Sharma and Owen,1996; Mehta and others, 2011), but may be lower for avalanche-fed or debris-covered glaciers (Kulkarni, 1992; Mehta and others, 2011). Field-based mass-balance measurements at Mera Glacier in the Khumbu region of Nepal indicate an average AAR of 0.58 at Mera Glacier from 2007 to 2013 (Wagnon and others, 2013). Remotely sensed imagery has also been used to estimate recent AARs that range between 0.30 and 0.76 in different regions of the HKH (Kääb and others, 2012; Gardelle and others, 2013).

To calculate dA/dELA, glacier hypsometries are first derived for each of the 76 HKH sub-basins using the Bajracharya and Shrestha (2011) glacier inventory and the Shuttle Radar Topography Mission (SRTM V4) gap-filled digital elevation model (DEM) at 90 m resolution (Farr and others, 2007). Higher-resolution DEMs are available, but not required for a regional-scale analysis. Estimates of ELA$_0$ are extracted from sub-basin glacier hypsometries using a range of AARs (0.40–0.60; Table 1). We then vary ELA$_0$ in 10 m increments, extract the resultant dA, and estimate dA/dELA within 100 m of ELA$_0$. Relations between glaciological sensitivity and characteristic glacier metrics (elevation range, mean slope, mean slope around the ELA, and total area) are explored to identify possible controlling parameters.

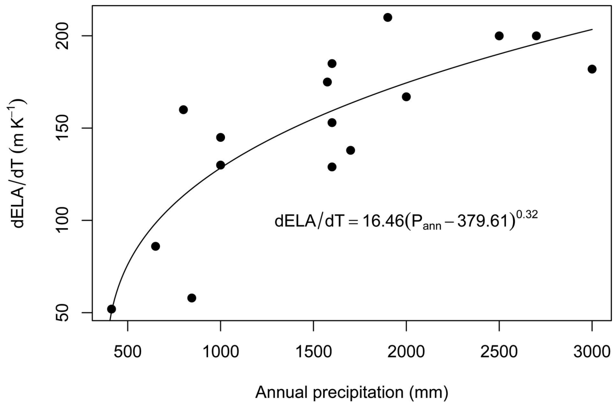

Fig. 1. ELA response to changes in temperature (dELA/dT) for sites with varying mean annual precipitation (data from Table 2).

The change in glacier area in response to a change in temperature can be expressed as a function of the glaciological sensitivity and the response of the ELA to changes in temperature:

$$\frac{\mathrm{d}A}{\mathrm{d}T} = \frac{\mathrm{d}A}{\mathrm{dELA}} \cdot \frac{\mathrm{dELA}}{\mathrm{d}T}. \quad (2)$$

dELA/dT depends primarily on the climatic setting. In general, glaciers in wetter regions have higher rates of mass turnover and experience higher temperatures, and are thus more sensitive to changes in temperature due to increased melt rates and changes in liquid/total precipitation ratios and ablation season lengths (Oerlemans and Fortuin, 1992). In the absence of other significant predictors, we derive a function to estimate dELA/dT from mean annual precipitation. We neglect here the possibly significant impact of debris cover on dELA/dT.

Our estimate of dELA/dT follows three main steps. Based on a compilation of observations, modeling studies, and paleo-ELA and climate studies from similar high-altitude regions (Table 2; Fig. 1), we first derive a function to estimate dELA/dT from mean annual precipitation. To estimate dELA/dT for all HKH sub-basins, mean annual precipitation from the High Asia Refined analysis (HAR) project (Maussion and others, 2014; Fig. 2) is then interpolated from 10 km resolution to 200 m resolution. Finally, the 200 m precipitation fields are clipped to the glacierized extents in each sub-basin, and used to estimate a mean dELA/dT.

Hydrological sensitivity

The sub-basin hydrological sensitivity is defined here as the change in glacier melt in response to increased temperature (dM/dT; m K^{-1}). Total ice melt (M) below the ELA is estimated as

$$M = \sum (Z - \mathrm{ELA}_0) \cdot \frac{\mathrm{d}M}{\mathrm{d}Z}, \quad (3)$$

where dM/dZ is the mass-balance gradient below ELA$_0$, Z is the gridcell elevation, and the summation is over all gridcells where $Z <$ ELA$_0$. Field-based and modeled mass-balance

https://doi.org/10.3189/2016AoG71A073 Published online by Cambridge University Press

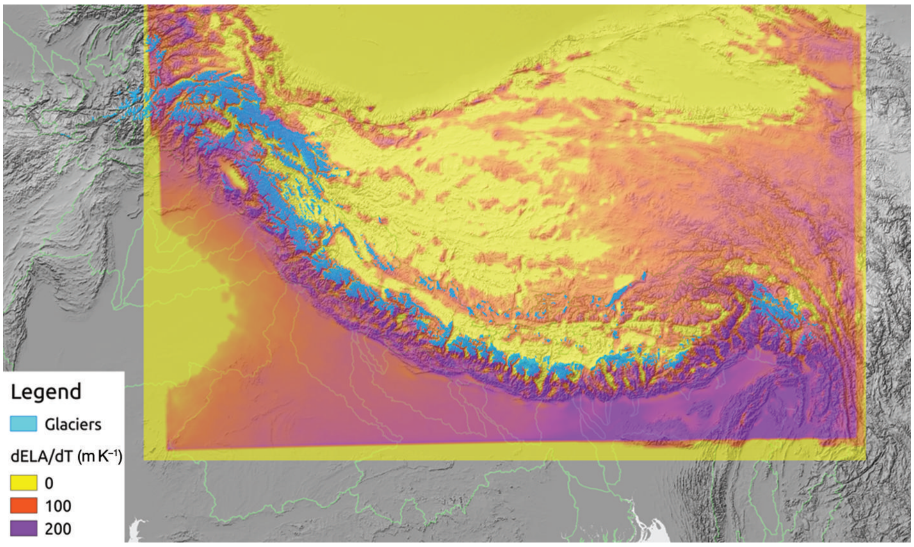

Fig. 2. Estimated dELA/dT based on Figure 1 and mean annual precipitation from Maussion and others (2014).

gradients reported in previous studies range between –0.4 and –1.5 m w.e. $(100\,m)^{-1}$ (Fujita and others, 1998; Konz and others, 2006; Wagnon and others, 2007, 2013; Racoviteanu and others, 2013; Shea and others, 2015). A dM/dZ range of –0.4 to –1.0 m w.e. $(100\,m)^{-1}$ (Table 1) is used to examine the uncertainty in our approach. More negative gradients are from small and lower-elevation glaciers that may not be representative of regional balance gradients.

In response to a change in temperature, we prescribe an increase in ELA that depends on mean annual precipitation over the glaciers in the sub-basin based on our estimates of dELA/dT. The change in ELA implies imbalance in the glacier geometry, and the rate at which a glacier can adapt to this new condition largely determines the hydrological sensitivities. Here we explore two bounding scenarios for basin responses to changes in ELA: (1) a static geometry where the total glacier area is left unchanged, or (2) an adjusted geometry, where the total glacier area is adjusted to reflect the loss of ice at lower elevations. The latter scenario is implemented by assuming that the glacier response to the new ELA is an instantaneous loss of mass and area at the lower elevations. The adjusted glacier hypsometry is calculated by iteratively removing area from the lowest elevations until the prescribed ELA corresponds to that indicated by a steady-state AAR.

Table 2. Sensitivity of ELA to changes in temperature (dELA/dT) and mean annual precipitation (P_{Ann}) for selected high-altitude sites

P_{Ann} mm	dELA/dT m K^{-1}	Location	Source
1600	153	Himalaya (AX010)	Shi and Liu (2000); Su and Shi (2002); Zhang and others (1998)
650	86	Urumqi Glacier No. 1, China	Zhang and others (1998)
413	52	July 1st (Qiyi) Glacier, China	Zhang and others (1998)
845	58	Tibetan Plateau (Dongkemadi)	Zhang and others (1998)
3000	182	Inner tropics (Lewis Glacier, Mount Kenya)	Kaser (2001)
1700	138	Colombia	Mark and Seltzer (2005)
2000	167	E. Andes (humid)	Klein and Isacks (1999)
1000	130	E. Andes (dry)	Klein and Isacks (1999)
2700	200	Ecuador	Sagredo and others (2014)
1000	145	Andes (N. mid-latitudes)	Sagredo and others (2014)
800	160	Andes (dry outer tropics)	Sagredo and others (2014)
2500	200	Patagonia	Sagredo and others (2014)
1600	185	S. outer tropics	Sagredo and others (2014)
1900	210	Andes (N. mid-latitudes)	Sagredo and others (2014)
1600	129	Venezuela Andes	Stansell and others (2007)
1575	175	Bhutan	Isacks and others (1995) in Owen and Benn (2005); Wangda and Ohsawa (2006)

This process is outlined in Figure 3. For the westerly-dominated Beas sub-basin of the Indus, the original hypsometry and assumed AAR of 0.5 give an $ELA_0 = 5016$ m. Based on mean annual precipitation of 1740 mm and an estimated dELA/dT of 164 m K^{-1}, a 1 K temperature increase will result in a new ELA of 5180 m. In the static geometry case, the glacier area remains unchanged, and the AAR is now ~0.20. In the adjusted geometry case, the lower elevations of the glacier are removed until the AAR returns to 0.5. Figure 3 also demonstrates this for the monsoon-dominated Dudh Koshi sub-basin of the Ganga. Low mean annual precipitation over the glaciers of the Dudh Koshi results in a reduced dELA/dT, and an ELA shift from 5516 m to 5613 m.

In this study the hydrological sensitivity to a +1 K warming is defined as (1) a percent change in total negative mass balance, and (2) a change in specific meltwater production (i.e. the change in meltwater production divided by the total glacierized area in the sub-basin). Both metrics are calculated for static and adjusted glacier geometries, and a range of assumptions about steady-state AAR and mass-balance gradient below the ELA are used to examine the effects on future glacier melt.

Glacier response time

To gain insight into the relation between the time period over which a climate change occurs and the actual retreat of a glacier, a first-order estimate of response time is made at the sub-basin scale. This approximation can be used to provide guidance for the lag between increased contributions in response to higher temperatures, and decreased glacier contributions in response to glacier retreat. We approximate the response times of glaciers in the region from the modeled thickness and mass-balance rate near the glacier terminus, following a method based on Jóhannesson and others (1989):

$$T_{\mathrm{R}} = \frac{-H'}{\dot{b}_{\mathrm{a}}} \tag{4}$$

where H' (m) is the maximum glacier thickness and $\dot{b}_{\mathrm{a}}$ ($\dot{b}_{\mathrm{a}} < 0$) is a mass-balance rate near the terminus. As ice thicknesses and terminus mass-balance rates are unknown, we test a range of modeled ice thicknesses and use a mean mass-balance rate below the ELA based on a regional geodetic study (Gardelle and others, 2013). Ice thicknesses are approximated for each sub-basin with a surface slope inversion and assumed basal shear stress (Immerzeel and others, 2012; Shea and others, 2015):

$$H = \frac{\tau_0}{\rho g \sin\beta} \tag{5}$$

where τ_0 is the assumed equilibrium shear stress (80 000 N m^{-2}), ρ is ice density (917 kg m^{-2}), g is gravitational acceleration and β is surface slope extracted from the 90 m SRTM DEM.

Neglecting advection of ice from upper elevations, we assume that annual surface mass loss rates near the terminus are -1.5 ± 0.5 m w.e. a^{-1}. This rate is based on the average surface lowering rates observed below the ELA in nine sub-regions of the HKH (cf. Gardelle and others, 2013, fig. 11). Basin-scale response times are then approximated from Eqn (5) with a range of values for H' based on the 10th, 50th and 90th percentiles of modeled ice depths below the hypsometry-derived ELA_0 (AAR = 0.5).

Our methods to generate first-order estimates of glaciological and hydrological responses at the sub-basin scale are limited by a number of necessary assumptions and generalizations. This approach is not expected to perform well at the scale of individual glaciers, but provides an important regional overview of future responses to climate change.

RESULTS

Glaciological sensitivity

High glaciological sensitivities indicate that the calculated ELA corresponds to a region with a proportionally large surface area. A small change in ELA will thus result in a large change in ablation area. Absolute increases in ablation areas (d*A*/dELA; km^2 (100 m)$^{-1}$) are greatest in the heavily glacierized catchments of the Upper Indus basin (Fig. 4), while the relative sensitivity (d*A*/dELA; % (100 m)$^{-1}$) shows greater spatial variability. The greatest relative sensitivities of ~20% (100 m)$^{-1}$ are observed on the northern side of the eastern Himalaya, and lower values are observed in the monsoon-dominated catchments.

At the sub-basin scale, glaciological sensitivity appears to be related primarily to the elevation range of glaciers in a given catchment (Fig. 5a). Sensitivities are also greatest for catchments with smaller glacierized areas (Fig. 5b). Mean glacier slope, calculated over all glacierized areas (Fig. 5c) and around the ELA (Fig. 5d), exhibits no strong relation with d*A*/dELA, though this is likely related to the aggregation of glaciers to the sub-basin scale. Large elevation ranges are an

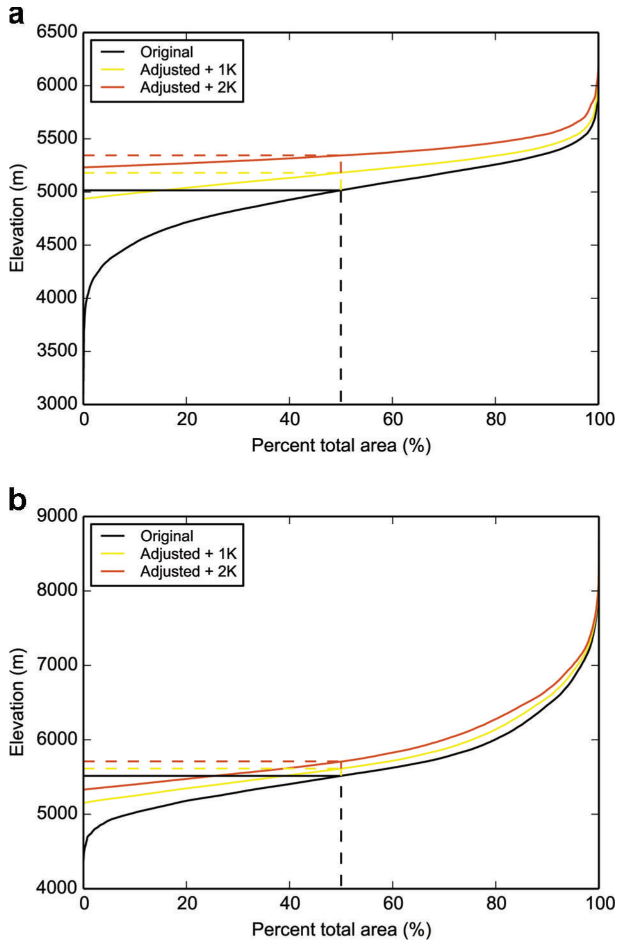

Fig. 3. ELAs, accumulation areas and basin-wide glacier hypsometries for original, static and adjusted geometry scenarios, assuming an AAR of 0.5 and a mass-balance gradient of –0.007 m m^{-1} below the ELA. Examples from (a) the westerly-dominated Beas basin, Indus River, and (b) the monsoon-dominated Dudh Koshi basin, Ganga River.

outcome of strong topographical relief and high accumulation rates that result in extensive glacier cover. In such climatic and topographic settings, changes in ablation area will be relatively insensitive to increases in ELA.

Our estimates of d*A*/dELA are subject to uncertainty due to the assumption of steady-state AAR (Fig. 6). The median sensitivity calculated for each basin changes ±1–2% depending on the AAR value used to estimate ELA_0; however, the maxima and minima can vary between 5% and 10%. There is no clear pattern as to whether a different AAR assumption increases or decreases the glaciological sensitivity.

Hydrological sensitivity

Static geometry

The assumption of a static glacier geometry would result in substantial increases in glacier melt for a 1 K warming (Fig. 7). With middle-of-the-road assumptions about AAR (0.5) and d*M*/d*Z* (–0.007 m w.e. m^{-1}), the average increase in meltwater yield is 40–50% K^{-1} for the Indus, Ganga and Brahmaputra basins. Some small basins on the Tibetan Plateau and in the Indus would see a doubling of meltwater yield if glacier geometries remain unchanged.

In the static geometry case, the AAR assumption has a direct and systematic effect on the percent increase in glacier meltwater (Fig. 8). In all basins, the assumption of a

https://doi.org/10.3189/2016AoG71A073 Published online by Cambridge University Press

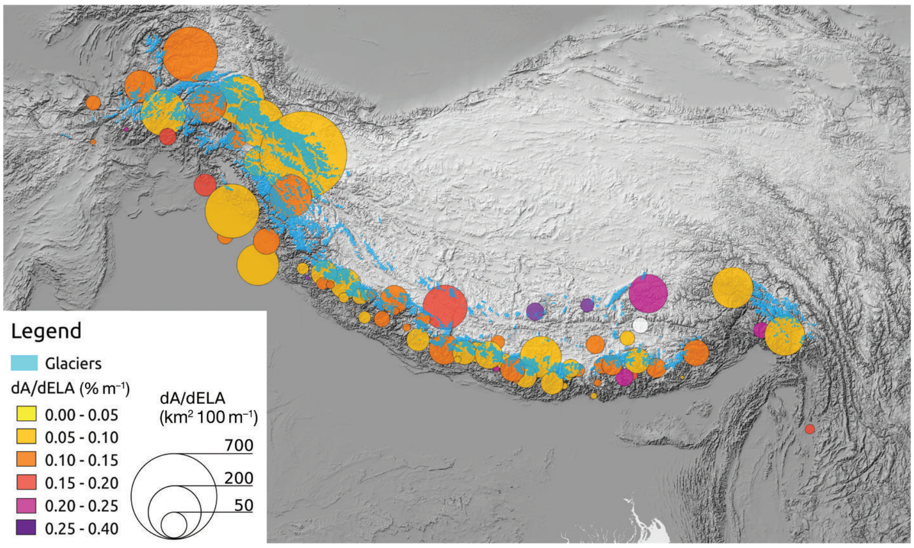

Fig. 4. Glaciological sensitivity (dA/dELA) of HKH sub-basins, expressed in relative (% m^{-1}; color scale) and absolute (km^2 (100 m)$^{-1}$; size of circle) measures.

larger AAR results in a greater percent increase in meltwater yield. While changes in the average basin meltwater yield are relatively insensitive to the assumed AAR, the maximum change in glacier-derived meltwater can increase by up to 150% depending on the assumed AAR (e.g. Ganga).

In terms of the magnitude of meltwater production increase with static glacier geometries, the assumed mass-balance gradient strongly affects future specific runoff (Fig. 8). More negative mass-balance gradients will result in substantial increases in meltwater production, with proportionally larger impacts on maximum sub-basin estimates. In the Indus basin, the average increase in unit meltwater production ranges from 0.30 to 0.76 m w.e. K^{-1} for mass-balance gradients of –0.004 to –0.011 m w.e. m^{-1},

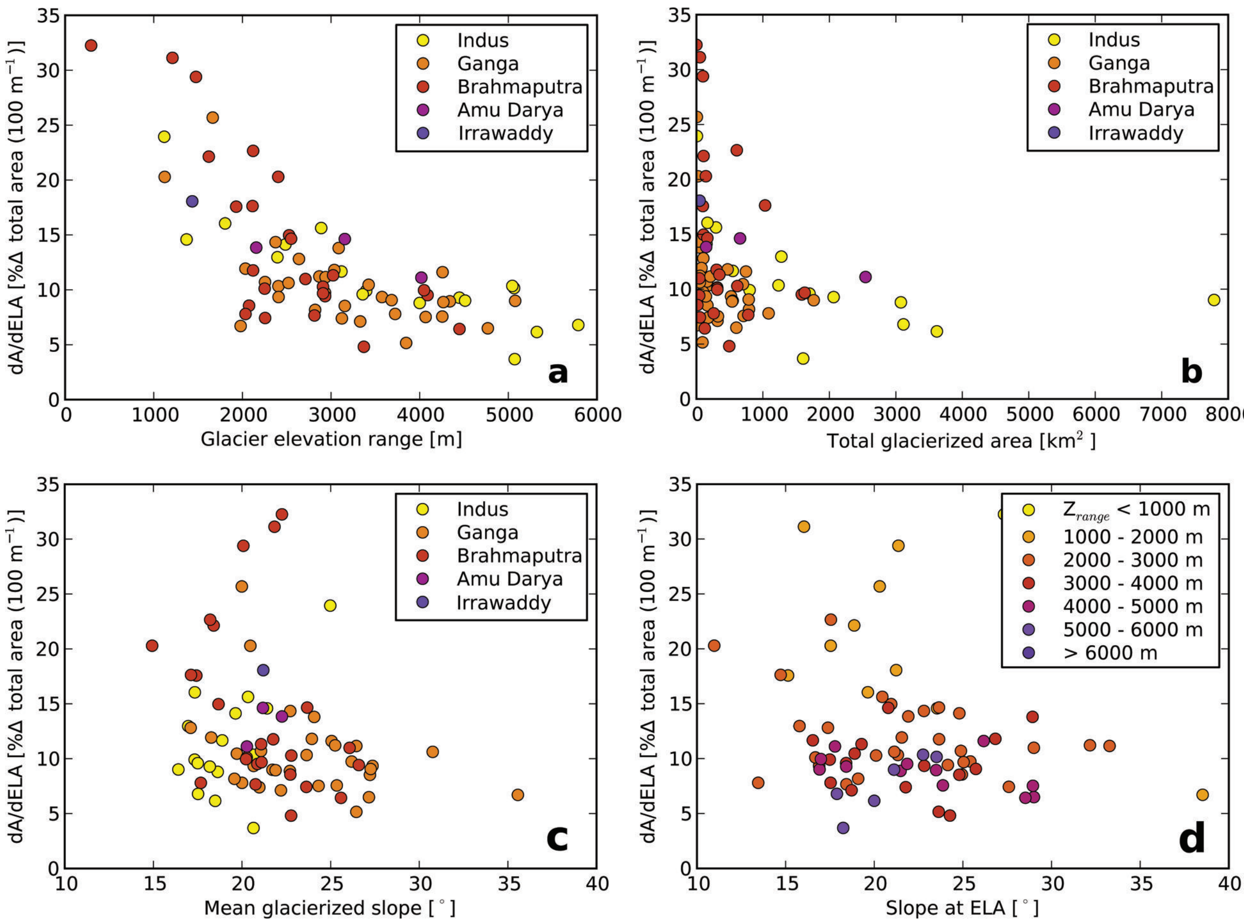

Fig. 5. Relations between relative glaciological sensitivity (dA/dELA; % (100 m)$^{-1}$) and (a) glacier elevation range, (b) total glacierized area, (c) mean glacierized slope and (d) glacierized slope at the ELA.

https://doi.org/10.3189/2016AoG71A073 Published online by Cambridge University Press

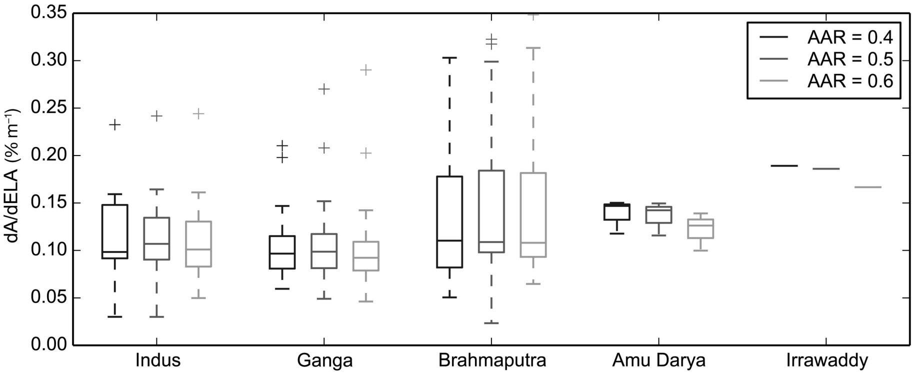

Fig. 6. Boxplots of calculated d*A*/dELA and sensitivity of steady-state AAR assumptions for the sub-basins in each major river basin. AAR = 0.4 is given in dark gray (left), AAR = 0.5 in medium gray (middle) and AAR = 0.6 in light gray (right) for each basin. No statistics are given for the Irrawaddy, which has only one glacierized sub-basin.

with an assumed steady-state AAR of 0.5. For the Ganga basin, sub-basin estimates of unit d*M*/d*T* range from 0.33 to 0.81 m w.e. K^{-1}, and for the Brahmaputra the range is from 0.24 to 0.59 m w.e. K^{-1}. For each basin, the maximum increase in unit meltwater production nearly doubles with each –0.003 decrease in d*M*/d*Z*.

Adjusted geometry

With instantaneous adjustments in glacier geometry in response to a +1 K warming, glacier runoff contributions decline in nearly all cases (Fig. 9). With AAR = 0.5 and $dM/dZ = -0.007$ m w.e. m^{-1}, mean glacier meltwater reductions in response to +1 K warming are greatest in the Indus River sub-basins, which show an average reduction of –64%, and a range between –14% and –86%. The Ganga and Brahmaputra sub-basins could see mean glacier meltwater reductions of –58% (–27% to –90%) and –57% (+14% to –87%), respectively. The lone sub-basin in the Brahmaputra that shows an increase in meltwater has a small glacierized area and atypical hypsometry.

With adjusted glacier geometries, the AAR assumption affects our estimates of glacier meltwater change (Fig. 10), but this effect is not systematic as observed for the static geometry case above. In some basins, lower estimates of AAR result in greater reductions in melt (e.g. Indus). For the Ganges, the mean reduction in meltwater is lowest when AAR = 0.5.

The assumed mass-balance gradient has a large impact on specific glacier runoff when the glacier geometry is fully adjusted (Fig. 10). In all cases, a more negative mass-balance gradient results in (1) greater adjustments to the glacier geometry and (2) greater reductions in the specific meltwater production. The greatest reductions in specific meltwater production are observed in the Indus and Ganga basins, with average (maximum) decreases between –0.4 (–0.75) and –1.0 (–2.0) m w.e.

Response times

While glacier mass balance responds directly to interannual climate variability, the geometric response (length, area) of glaciers to climate change will occur on timescales ranging

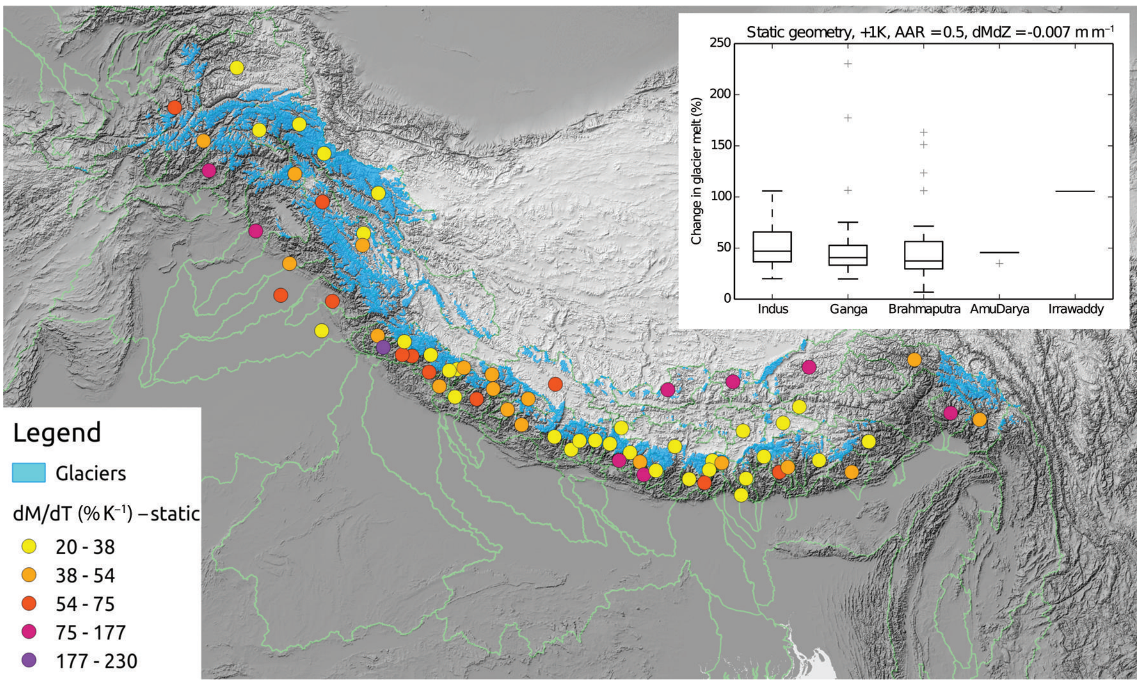

Fig. 7. Percent change in glacier melt for +1 K temperature increase (d*M*/d*T*) in HKH sub-basins, estimated using AAR = 0.5, static glacier geometries, and a mass-balance gradient of –0.007 m w.e. m^{-1}. Inset graph shows basin boxplots of d*M*/d*T*.

https://doi.org/10.3189/2016AoG71A073 Published online by Cambridge University Press

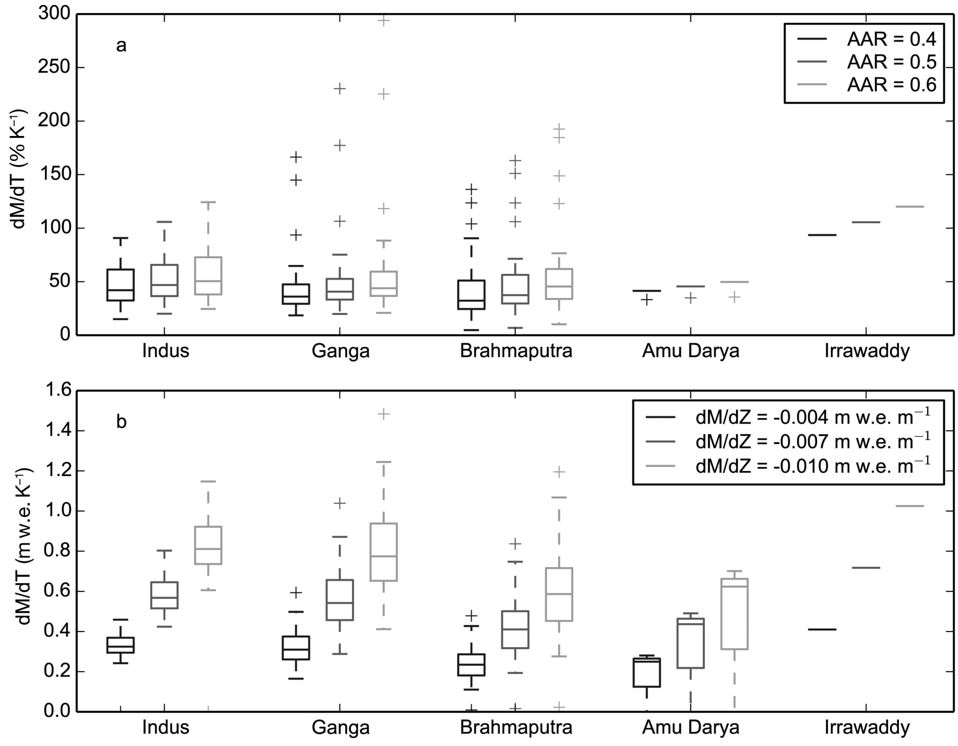

Fig. 8. Boxplots of hydrological sensitivities to AAR and mass-balance gradient with static glacier geometry. (a) Sensitivity of percent change in glacier contribution (% K^{-1}) to assumptions of steady-state AAR, for +1 K increase in temperature (assumed $dM/dZ = -0.007$ m w.e. m^{-1}). (b) Sensitivity of specific glacier meltwater production (m w.e. m^{-1}) to mass-balance gradient (assumed AAR = 0.5).

from decades to centuries. To place our bounding scenarios of static geometry and instantaneous glacier change in context, we develop first-order estimates of glacier response times at the sub-basin scale. A glacier response time is defined as the e-folding timescale for a glacier to move from one steady state to another in response to an imposed step change in climate (Cogley and others, 2011).

At the sub-basin scale, glacier response times vary greatly depending on the input data (Fig. 11), and we caution that our estimates here are to be used only for guidance. With a low estimate of glacier thickness (10th percentile), mean response times vary from 11 ± 3 to 12 ± 4 years (Table 3). The error terms reported here are the standard deviations among all sub-basins, based on the rough approximations of

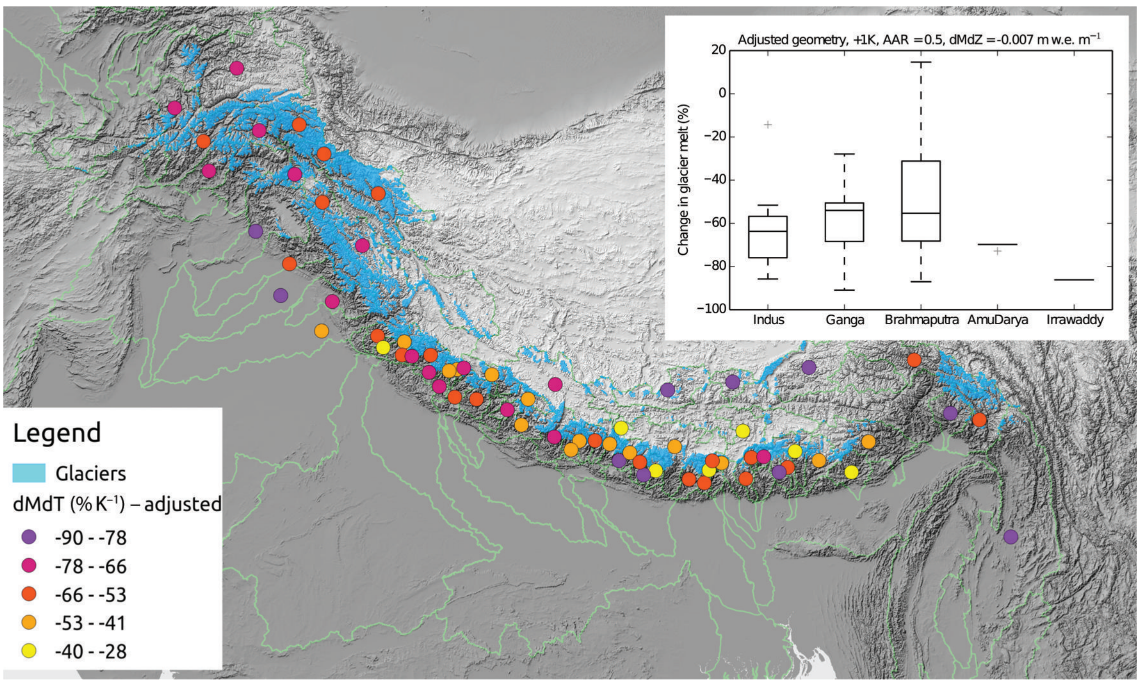

Fig. 9. Percent change in glacier melt for +1 K temperature increase (dM/dT) in HKH sub-basins, estimated using AAR = 0.5, adjusted glacier geometries and a mass-balance gradient of –0.007 m w.e. m^{-1}. Inset graph shows basin boxplots of dM/dT. Glacier melt is reduced in (nearly) all cases.

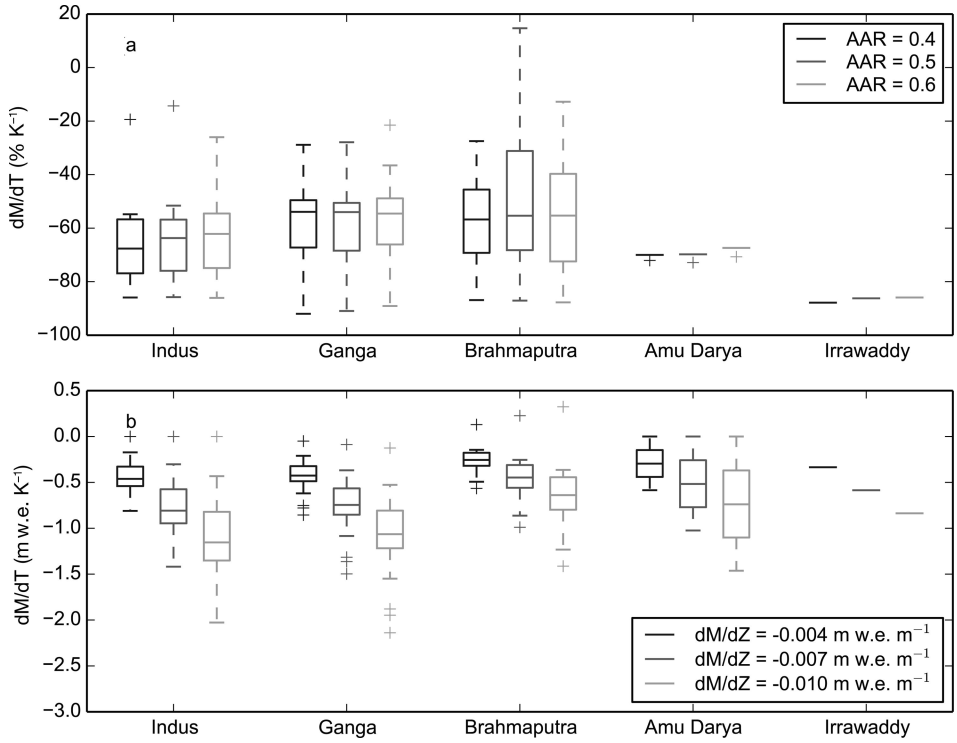

Fig. 10. Boxplots of hydrological sensitivities to AAR and mass-balance gradient with adjusted glacier geometry. (a) Sensitivity of percent change in glacier contribution to assumptions of steady-state AAR, for +1 K increase in temperature (assumed dM/dZ = –0.007 m w.e. m^{-1}). (b) Sensitivity of specific glacier meltwater production to mass-balance gradient (assumed AAR = 0.5).

mass change rates near the terminus (Gardelle and others, 2013). Response times calculated using a median modeled thickness range between 18 ± 5 and 31 ± 14 years. More conservative estimates of response time, based on the 90th percentile of modeled glacier thickness, give a range between 36 ± 10 and 95 ± 52 years. Approximated response times are greatest in the Indus basin, and lowest in the Irrawaddy.

When compared with potential conservative rates of warming (+1 K by 2050, or +1 K by 2100), the response times give an approximation of sub-basins that might be experiencing increased or reduced streamflows (Table 3). Using the most conservative estimate of T_R based on 90th percentile of modeled ice depths, we find that most sub-basins will still be experiencing increased glacier contributions at 2050. However, by 2100 at least half and potentially all of the sub-basins in the region could see reduced glacier contributions. As distributed modeling studies have found (e.g. Immerzeel and others, 2013; Lutz and others, 2014), glacier contributions to streamflow start to decline in the second half of the 21st century. Using our simple geometrical approach we arrive at a similar conclusion.

DISCUSSION AND CONCLUSIONS

Water resources in the HKH region are derived from precipitation, snowmelt and glacier melt. Through a broad analysis that incorporates current glacier distributions and assumptions about (1) steady-state AAR, (2) mass-balance gradients and (3) the ELA responses to temperature change, we analyse the sensitivity of glaciers and glacier contributions to streamflow at the sub-basin scale. Glaciers will

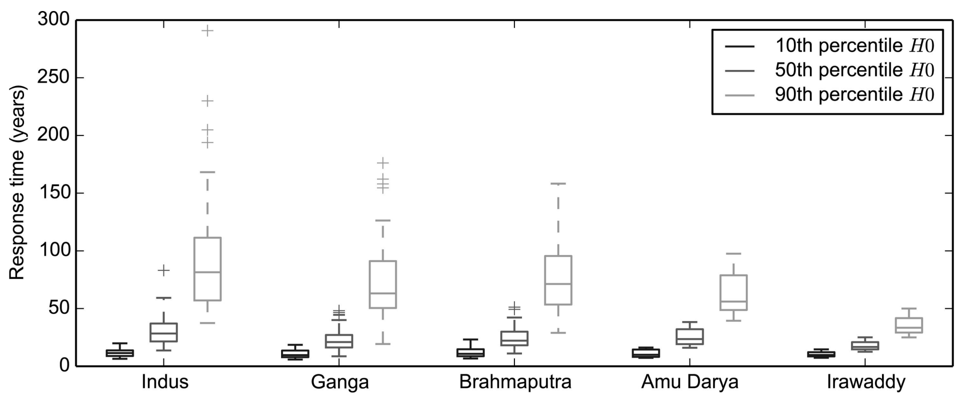

Fig. 11. Boxplots of approximated glacier response times. For each basin the range of sub-basin T_R is shown, calculated with (left) the 10th percentile of modeled ice depth, (middle) the median and (right) the 90th percentile. The range includes variability due to our estimate of mass loss near the terminus (-1.5 ± 0.5 m a^{-1}).

https://doi.org/10.3189/2016AoG71A073 Published online by Cambridge University Press

Table 3. Response times approximated from modeled ice thicknesses below the ELA (10th, 50th and 90th percentiles) and terminus melt rates of -1.5 ± 0.5 m w.e. a^{-1}. Also shown are the percentage of sub-basins where glaciers might be fully adjusted, i.e. where T_R is <35 years (+1 K warming at 2050), and <85 years (+1 K at 2100)

Basin$_n$	T_R years	$T_R < 35$ %	$T_R < 85$ %
Indus$_{10}$	11.9 ± 3.8	100.0	100.0
Indus$_{50}$	31.2 ± 13.7	66.7	100.0
Indus$_{90}$	94.9 ± 51.8	0.0	52.9
Ganga$_{10}$	10.7 ± 3.3	100.0	100.0
Ganga$_{50}$	22.7 ± 8.8	89.2	100.0
Ganga$_{90}$	72.7 ± 32.0	7.5	71.0
Brahmaputra$_{10}$	11.8 ± 3.8	100.0	100.0
Brahmaputra$_{50}$	24.6 ± 8.9	86.7	100.0
Brahmaputra$_{90}$	77.4 ± 32.0	5.3	67.0
Amu Darya$_{10}$	11.0 ± 3.2	100.0	100.0
Amu Darya$_{50}$	25.4 ± 7.6	77.7	100.0
Amu Darya$_{90}$	62.7 ± 19.0	0.0	88.0
Irrawaddy$_{10}$	10.6 ± 3.0	100.0	100.0
Irrawaddy$_{50}$	18.1 ± 5.2	100.0	100.0
Irrawaddy$_{90}$	36.1 ± 10.4	67.0	100.0

produce increased runoff in response to increased temperatures, with a +1 K warming producing up to 200% increases in ice melt in some cases. However, increased ice mass loss will lead to changes in glacier area and volume, and reductions in ice melt. It is unclear how quickly basins will move towards peak water and onward to reduced flows, but our approximations of glacier response times suggest that most basins will see reduced glacier contributions to streamflow by 2100. Such reductions in glacier runoff will be particularly important in basins where glacier-derived meltwater is a critical source of streamflow during dry periods.

Previous studies examining hydrological responses to glacier change have either neglected the glacier response (Fukushima and others, 1991; Singh and Bengtsson, 2004), used volume–area scaling approaches (Van de Wal and Wild, 2001; Stahl and others, 2008; Bliss and others, 2014) to adjust glacier extents, or have used simplified models of glacier dynamics to account for glacier change (Lutz and others, 2014). The assumption of no glacier change results in greater modeled discharges with increased temperatures, as our study also demonstrates (Fig. 8). Higher-complexity approaches to modeling the effects of increased temperatures on glaciers are limited by the availability of input data, and volume–area scaling approaches are subject to considerable uncertainty (Radić and Hock, 2010). Our approach provides an alternate method by placing bounds on the glaciological and thus hydrological responses.

Our methods to estimate glaciological and hydrological sensitivity rely on a number of assumptions, which we examine below. First, our approach aggregates glaciers to the sub-basin scale, while the response of individual glaciers will be based on local slope, aspect, topography and debris cover (Anderson, 2012). Debris cover, in particular, acts to reduce the mass-balance sensitivity, and basins with higher concentrations of debris-covered glaciers might be expected to have a reduced dELA/dT sensitivity. Debris-cover extents and thicknesses are largely unknown in the HKH, and these factors would be key to quantifying the reduced dELA/dT sensitivity. Currently, it is unclear how to incorporate debris cover into our regional-scale analysis, and an understanding of the impacts of glacier change for downstream water resources requires an aggregated approach.

Second, our scenarios of either (1) static geometry or (2) instantaneous fully adjusted geometry are both incorrect, and are intended to represent upper and lower bounds on the glaciological and hydrological changes. In reality, the response of glacier geometry to increased melt will be complex and time-varying, and different for individual glaciers. Our estimated response times vary greatly depending on the methods used, but are instructive for assessing which basins will see rapid adjustments to warming, and which will reach peak water at later dates.

Third, our analysis rests upon the assumed relation between dELA/dT and mean annual precipitation. Three of the studies used are based on reconstructed ELAs and assumed temperature changes, which are subject to errors related to the propagation of age uncertainties. There are, furthermore, a number of different methods for estimating paleo-ELAs (Benn and Lemkuhl, 2000), and the precipitation values assigned to each data point in Figure 1 are uncertain. Consequently, there exists a large range of possible parameter values for the function that relates dELA/dT and mean annual precipitation. Nevertheless, the relation between mean annual precipitation and dELA/dT is derived primarily from high-altitude sites where the climatic differences are relatively small. A greater range of observational and/or modeling studies to constrain the parameter values in this function would lend greater confidence to the approach we have used.

The derived relationship between dELA/dT and mean annual precipitation (Fig. 1) is consistent with the observation of Oerlemans and Fortuin (1992) that glaciers in wetter climates are more sensitive to temperature changes. Mass-balance gradients are also steeper in wetter regions due to the generally higher temperatures that lead to higher rates of mass turnover (e.g. Raper and Braithwaite, 2006). Global glacier mass-balance models further suggest that glaciers in maritime regions (e.g. Scandinavia and New Zealand) tend to have a greater sensitivity to temperature changes (Marzeion and others, 2012; Radić and others, 2014).

Fourth, we examine the uncertainty in our approach based on AAR and dM/dZ assumptions, but we do not consider the effects of debris cover or avalanche nourishment on glacier response. We also do not consider future changes in precipitation. Climate models show uncertainty in both the sign and magnitude of projected precipitation changes in the region, which reflects the uncertainty of monsoon responses to climate change.

Finally, our estimates of response times are highly uncertain, and are intended to be used for guidance only. The response times of individual glaciers will be highly variable, and it is not clear that the approach of Jóhannesson and others (1989) can be adapted for all glaciers in a sub-basin. There are also alternative approximations of ice depth (e.g. Huss and Farinotti, 2012) that may give improved response-time estimates, but as these are linked to specific glaciers in the Randolph Glacier Inventory (Pfeffer and others, 2014) they were not compatible with the sub-basin approach we used here. Neither method for estimating ice thickness can be validated in this data-poor region, and the gridded method used here was adapted easily for our study. We have

https://doi.org/10.3189/2016AoG71A073 Published online by Cambridge University Press

provided a range of response time estimates, and suggest that the 90th percentile of modeled ice depths gives the most reasonable (and conservative) estimate of response times.

At the regional scale, our approach indicates that initial increases in glacier contributions to streamflow will occur across the region in response to increased temperatures. However, a majority of sub-basins in the HKH region will see declines in glacier contributions to streamflow as a result of sustained warming, and this key result is consistent with distributed modeling approaches (Immerzeel and others, 2012; Lutz and others, 2014). These declines will likely occur on decadal to century timescales, and will impact water availability in basins where glacier contributions to streamflow are critical.

ACKNOWLEDGEMENTS

This study was partially supported by core funds of the International Centre for Integrated Mountain Development (ICIMOD) contributed by the Governments of Afghanistan, Austria, Bangladesh, Bhutan, China, India, Myanmar, Nepal, Norway, Pakistan, Switzerland and the United Kingdom. The ICIMOD Cryosphere Initiative is funded by the Norwegian Ministry of Foreign Affairs. The views and interpretations in this publication are those of the authors and are not necessarily attributable to ICIMOD. We thank the Scientific Editor Lindsey Nicholson, Francesca Pellicciotti, Patrick Wagnon and two anonymous reviewers for constructive comments on earlier versions of this work.

REFERENCES

Anderson B (2012) Controls on mass balance sensitivity of maritime glaciers in the Southern Alps, New Zealand: the role of debris-cover. *J. Geophys. Res.*, **117**, F01003

Bajracharya SR and Shrestha B eds (2011) *The status of glaciers in the Hindu Kush–Himalayan region*. International Centre for Integrated Mountain Development, Kathmandu http://lib.icimod.org/record/9419/files/icimod-the_status_of_glaciers_in_the_hindu_kush-himalayan_region%5B1%5D.pdf.

Baraer M and 8 others (2012) Glacier recession and water resources in Peru's Cordillera Blanca. *J. Glaciol.*, **58**, 134–150

Benn DI and Lemkuhl F (2000) Mass balance and equilibrium-line altitudes of glaciers in high-mountain environments. *Quat. Int.*, **65**, 15–29

Bliss A, Hock R and Radić V (2014) Global response of glacier runoff to twenty-first century climate change. *J. Geophys. Res. Earth Surf.*, **119**, 717–730

Bolch T and 11 others (2012) The state and fate of Himalayan glaciers. *Science*, **336**, 310–314

Brun F and 8 others (2014) Seasonal changes in surface albedo of Himalayan glaciers from MODIS data and links with the annual mass balance. *Cryosphere Discuss.*, **8**(3), 3437–3474

Burbank DW and Cheng KJ (1991) Relative dating of Quaternary moraines, Rongbuk valley, Mount Everest, Tibet: implications for an ice sheet on the Tibetan Plateau. *Quat. Res.*, **36**, 1–18

Cogley JG and 10 others (2011) *Glossary of glacier mass balance and related terms*. (IHP-VII Technical Documents in Hydrology No. 86, IACS Contribution No. 2) UNESCO–International Hydrological Programme

Farr TG and 17 others (2007) The Shuttle Radar Topography Mission. *Rev. Geophys.*, **45**, 2004

Fujita K, Takeuchi N and Seko K (1998) Glaciological observations of Yala Glacier in Langtang Valley, Nepal Himalayas, 1994 and 1996, *Bull. Glacier Res.*, **16**, 75–81

Fukushima Y, Watanabe O and Higuchi K (1991) Estimation of streamflow change by global warming in a glacier-covered high mountain area of Nepal Himalaya. *IAHS Publ.* 205 (Symposium at Vienna 1991 – *Snow, Hydrology and Forests in High Alpine Areas*), 181–188

Gardelle J, Berthier E, Arnaud Y and Kääb A (2013) Region-wide glacier mass balances over the Pamir–Karakoram–Himalaya during 1999–2011. *Cryosphere*, **7**, 1263–1286

Hewitt K (2005) The Karakoram anomaly? Glacier expansion and the 'elevation effect', Karakoram Himalaya. *Mt. Res. Dev.*, **25**(4), 332–340

Huss M and Farinotti D (2012) Distributed ice thickness and volume of all glaciers around the globe. *J. Geophys. Res.: Earth Surf.*, **117**, 4010

Huss M, Zemp M, Joerg PC and Salzmann N (2014) High uncertainty in 21st century runoff projections from glacierized basins. *J. Hydrol.*, **510**, 35–48

Immerzeel WW, Van Beek LPH and Bierkens MFP (2010) Climate change will affect the Asian water towers. *Science*, **328**, 1382–1385

Immerzeel WW, Van Beek LPH, Konz M, Shrestha AB and Bierkens MFP (2012) Hydrological response to climate change in a glacierized catchment in the Himalayas. *Climatic Change*, **110**, 721–736

Immerzeel WW, Pellicciotti F and Bierkens MFP (2013) Rising river flows throughout the twenty-first century in two Himalayan glacierized watersheds. *Nature Geosci.*, **6**(9), 742–745

Isacks BL, Duncan C and Klein AG (1995) Modern and LGM glacial extents from satellite images and digital topography: implications for LGM climate in the Bhutan Himalaya. *International Himalayan/Tibetan Plateau Paleoclimate Workshop – Abstracts*. Kathmandu

Jacob T, Wahr J, Pfeffer WT and Swenson S (2012) Recent contributions of glaciers and ice caps to sea level rise. *Nature*, **482**, 514–518

Jóhannesson T, Raymond C and Waddington E (1989) Time-scale for adjustment of glaciers to changes in mass balance. *J. Glaciol.*, **35**, 355–369

Kääb A, Berthier E, Nuth C, Gardelle J and Arnaud Y (2012) Contrasting patterns of early twenty-first-century glacier mass change in the Himalayas. *Nature*, **488**(7412), 495–498

Kaser G (2001) Glacier–climate interaction at low latitudes. *J. Glaciol.*, **47**, 195–204

Klein AG and Isacks BL (1999) Spectral mixture analysis of Landsat thematic mapper images applied to the detection of the transient snowline on tropical Andean glaciers. *Global Planet. Change*, **22**(1), 139–154

Konz M, Uhlenbrook S, Braun L, Shrestha A and Demuth S (2006) Tradeoffs for the implementation of a process-based catchment model in a poorly gauged, highly glacierized Himalayan headwater. *Hydrol. Earth Syst. Sci. Discuss.*, **3**, 3473–3515

Kuhn M (1989) The response of the equilibrium line altitude to climate fluctuations: theory and observations. In Oerlemans J ed. *Glacier fluctuations and climatic change*. Kluwer Academic Press, Dordrecht, 407–417

Kulkarni AV (1992) Mass balance of Himalayan glaciers using AAR and ELA methods. *J. Glaciol.*, **38**, 101–104

La Frenierre J and Mark BG (2014) A review of methods for estimating the contribution of glacial meltwater to total watershed discharge. *Progr. Phys. Geogr.*, **38**(2), 173–200

Lutz AF, Immerzeel WW, Shrestha AB and Bierkens MFP (2014) Consistent increase in High Asia's runoff due to increasing glacier melt and precipitation, *Nature Climate Change*, **4**, 587–592

Mark BG and Seltzer GO (2005) Evaluation of recent glacier recession in the Cordillera Blanca, Peru (AD 1962–1999): spatial distribution of mass loss and climatic forcing. *Quat. Sci. Rev.*, **24**, 2265–2280

Marshall SJ and 7 others (2011) Glacier water resources on the eastern slopes of the Canadian Rocky Mountains. *Can. Water Res. J.*, **36**(2), 109–134

Marzeion B, Jarosch AH and Hofer M (2012) Past and future sea-level change from the surface mass balance of glaciers. *Cryosphere*, **6**, 1295–1322

https://doi.org/10.3189/2016AoG71A073 Published online by Cambridge University Press

Maussion F, Scherer D, Mölg T, Collier E, Curio J and Finkelnburg R (2014) Precipitation seasonality and variability over the Tibetan Plateau as resolved by the High Asia Reanalysis. *J. Climate*, **27**, 1910–1927

Mehta M, Dobhal DP and Bisht MPS (2011) Change of Tipra glacier in the Garhwal Himalaya, India, between 1962 and 2008. *Progr. Phys. Geogr.*, **35**(6), 721–738

Meier MF (1962) Proposed definitions for glacier mass budget terms. *J. Glaciol.*, **4**, 252–261

Oerlemans J and Fortuin JPF (1992) Sensitivity of glaciers and small ice caps to greenhouse warming. *Science*, **258**(5079), 115–117

O'Neel S, Hood E, Arendt A and Sass L (2014) Assessing streamflow sensitivity to variations in glacier mass balance. *Climatic Change*, **123**(2), 329–341

Owen L and Benn D (2005) Equilibrium-line altitudes of the Last Glacial Maximum for the Himalaya and Tibet: an assessment and evaluation of results. *Quat. Int.*, **138**, 55–78

Pfeffer WT and 18 others (2014) The Randolph Glacier Inventory: a globally complete inventory of glaciers. *J. Glaciol.*, **60**, 537–552

Porter SC (1970) Quaternary glacial record in Swat Kohistan, West Pakistan. *Geol. Soc. Am. Bull.*, **81**, 1421

Rabatel A, Dedieu JP and Vincent C (2005) Using remote-sensing data to determine equilibrium-line altitude and mass-balance time series: validation on three French glaciers, 1994–2002. *J. Glaciol.*, **51**, 539–546

Racoviteanu AE, Armstrong R and Williams MW (2013) Evaluation of an ice ablation model to estimate the contribution of melting glacier ice to annual discharge in the Nepalese Himalaya. *Water Resour. Res.*, **49**, 5117–5133

Radić V and Hock R (2010) Regional and global volumes of glaciers derived from statistical upscaling of glacier inventory data. *J. Geophys. Res.: Earth Surf.*, **115**, F01010

Radić V, Bliss A, Beedlow AC, Hock R, Miles E and Cogley JG (2014) Regional and global projections of twenty-first century glacier mass changes in response to climate scenarios from global climate models. *Climate Dyn.*, **42**, 37–58

Raper SCB and Braithwaite RJ (2006) Low sea level rise projections from mountain glaciers and icecaps under global warming. *Nature*, **439**, 311–313

Sagredo EA, Rupper S and Lowell TV (2014) Sensitivities of the equilibrium line altitude to temperature and precipitation changes along the Andes. *Quat. Res.*, **81**, 355–366

Sharma MC and Owen LA (1996) Quaternary glacial history of NW Garhwal, Central Himalayas. *Quat. Sci. Rev.*, **15**, 335–365

Shea JM, Menounos B, Moore RD and Tennant C (2013) An approach to derive regional snow lines and glacier mass change from MODIS imagery, western North America. *Cryosphere*, **7**, 667–680

Shea JM, Immerzeel WW, Wagnon P, Vincent C and Bajracharya S (2015) Modelling glacier change in the Everest region, Nepal Himalaya. *Cryosphere*, **9**, 1105–1128

Shi YF and Liu SY (2000) Estimation on the response of glaciers in China to the global warming in the 21st century. *Chinese Sci. Bull.*, **45**(7), 668–672

Singh P. and L. Bengtsson (2004) Hydrological sensitivity of a large Himalayan basin to climate change. *Hydrol. Process.*, **18**, 2363–2385

Sorg A, Bolch T, Stoffel M, Solomina O and Beniston M (2012) Climate change impacts on glaciers and runoff in Tien Shan (Central Asia). *Nature Climate Change*, **2**(10), 725–731

Stahl K and Moore RD (2006) Influence of watershed glacier coverage on summer streamflow in British Columbia, Canada. *Water Resour. Res.*, **42**, W06201

Stahl K, Moore RD, Shea JM, Hutchinson D and Cannon AJ (2008) Coupled modelling of glacier and streamflow response to future climate scenarios. *Water Resour. Res.*, **440**, W02422

Stansell ND, Polissar PJ and Abbott MB (2007) Last Glacial Maximum equilibrium-line altitude and paleo-temperature reconstructions for the Cordillera de Mérida, Venezuelan Andes. *Quat. Res.*, **67**, 115–127

Su Z and Shi Y (2002) Response of monsoonal temperate glaciers to global warming since the Little Ice Age. *Quat. Int.*, **97**, 123–131

Van de Wal RSW and Wild M (2001) Modelling the response of glaciers to climate change by applying volume–area scaling in combination with a high resolution GCM. *Climate Dyn.*, **18**, 359–366

Wagnon P and 10 others (2007) Four years of mass balance on Chhota Shigri Glacier, Himachal Pradesh, India, a new benchmark glacier in the western Himalaya. *J. Glaciol.*, **53**, 603–611

Wagnon P and 11 others (2013) Seasonal and annual mass balances of Mera and Pokalde glaciers (Nepal Himalaya) since 2007. *Cryosphere*, **7**(4), 1769–1786

Wangda P and Ohsawa M (2006) Gradational forest change along the climatically dry valley slopes of Bhutan in the midst of humid eastern Himalaya. *Plant Ecol.*, **186**(1), 109–128

Williams VS (1983) Present and former equilibrium-line altitudes near Mount Everest, Nepal and Tibet. *Arct. Alp. Res.*, 201–211

Xu J and 6 others (2009) The melting Himalayas: cascading effects of climate change on water, biodiversity, and livelihoods. *Conserv. Biol.*, **23**(3), 520–530

Zhang Y, Yao T and Pu J (1998) The response of continental-type glaciers to climate change in China. *J. Glaciol. Geocryol.*, **20**(1), 3–8